

# Investigation of the Pressure Drop and Heat Transfer by Axially Grooving the Inner Surface of a Circular Tube Using Computational Fluid Dynamics

Md. Motiur Rahman,<sup>a)</sup> Dr Debasish Sarker,<sup>b)</sup> and Tanbin Mahmud<sup>c)</sup>

*Department of Mechanical Engineering,  
College of Engineering and Technology  
International University of Business Agriculture and Technology  
Dhaka, Bangladesh*

<sup>a)</sup>Corresponding author: bari.rahman97@gmail.com

<sup>b)</sup>dsarker.me@iubat.edu

<sup>c)</sup>tanbinmahmud@gmail.com

**Abstract.** Numerous heating and cooling procedures across several sectors make use of heat exchangers. The fluid's flow and heat-transfer characteristics inside the heat exchanger tube have an impact on the efficiency of the device. This study analyses the flow and heat transfer characteristics of water within a straight circular tube with axially grooved inner surface. For this investigation, a 3D numerical model for straight circular pipe of 11.08 mm diameter and 1920 mm length was developed with water as the heat transfer fluid and validated using published experimental data. The simulation was done for a range of Reynolds numbers (1500 – 23,000) and with four axial grooving of (1 mm × 0.5 mm) on the inner surface of tube. The results revealed that the axial grooving in the inner surface of the tube significantly increases the heat transfer between 2% and 10%. The pressure drop along the tube also slightly increased between 0.1% and 1.6%. The overall efficiency increases between 5% and 12% by using inner surface grooved tube.

**Keywords:** Forced convection, Axially grooved circular tube, Rectangular groove, Numerical heat transfer

## INTRODUCTION

Heat exchangers are utilized for both heating and cooling in a variety of industrial processes. The turbulator is one method of augmenting heat transfer. To boost the heat performance rate, various turbulators are frequently used on heat exchangers in the industry. The fluid flow field and the local heat transfer coefficient are altered by different turbulator arrangements. These modifications will result in a notable shift in the pressure drop and an increase in the rate of heat transfer. Consequently, the design of the heat exchangers tube is influenced by the turbulator configuration. Throughout the last decades, passive enhancement techniques such as adding a turbulator or changing the tubes by adding a groove are commonly utilized for heat exchangers to increase the heat transfer rate. This approach is simple to implement and doesn't require any additional power sources for the existing heat exchanger [7].

Numerous turbulators have been used in circular tubes to enhance convective heat transfer. A number of turbulator has been investigated by researchers, such as dimple, corrugated grooving [4], twisted tape [1, 3], wire coil [9, 13], and wing [11].

Eiamsa-ard and Promvong [10] have reported on a numerical investigation into turbulent flows in the periodically grooved channels in 2D with a range of Reynolds numbers 6000 – 18,000 and the (B/H) of 0.5 – 1.75. They discovered that the grooved tube enhances the heat transfer up to 158% in contrast with the smooth tube. The maximum gain of 1.33 on factor for thermal performance is acquired for the particular of groove-width to the channel-height proportion by roughly 0.75. Bilen et al. [8] experimentally research the influence of developed turbulent air flow in different tubes with grooves for Reynolds number varying between 10,000 and 38,000 with various geometric groove shapes, such as circular, trapezoidal, and rectangular. They discovered an optimal value of Reynolds number 17,000 for entropy generation. The heat transfer effectiveness for all pipes with a groove was acquired up to 1.28 for the circular groove, 1.25 was for the trapezoidal groove, and 1.26 for the rectangular groove. Wu and Zhou [14] numerically investigated the fluid flow for corrugated pipes with the range of value between 0.88 – 1.15 for (p/D) and 0.05–0.02 for (e/D), the Reynolds number vary between  $10^6$  –  $10^8$ . The results indicated that the corrugation/groove height enhances the heat transfer. Mesgarpour et al. [12] numerically investigated the enhancement of the thermal efficiency for various grooved tubes, for a range of Reynolds number between 500 and 2000. Ionanofluid was used as working fluid with a concentration of 0.05% – 2%. Results showed that for the spirally corrugated/grooved tube, the heat

transfer coefficient increases by 15.54% with 0.05% concentration of ionanofluid with compression to the smooth tube at Re about 500. Al-obaidi et al. [5] used interrupted axial groove patterns to alter the structure of flow in a circular tube with varying Reynolds number ranging between 1500 and 23000. Consequently a higher performance in terms of Nusselt number between 14.5% and 21% was detected for the grooved tube in contrast to the smooth tube. Considering the earlier studies, It is evident that using turbulators in cooling for electronic equipment and heat exchangers are extensively used in numerous heat exchanging fields. Using these new devices can improve mixing flow and vortex flow, which consequently leads to the improvement of overall heat transfer.

Though most of the studies focuses on improving the heat transfer by using various turbulator devices mostly flow obstacle devices, which improves the heat transfer but with the cost of added pressure drop. Which indicates that the overall efficiency of these devices are not improved and in some cases efficiency drops due to increasing pressure drop. This present study is focused on improving the heat transfer, but not for the cost of increased pressure drop. In this study we didn't use any flow restricting devices rather than we cut four small axial grooves at the inner surface of the tube to increase the area for the heat transfer. The axial grooves are in the same direction of the fluid flow therefore, there was no added pressure loss, only frictional loss due to increased area. In this following study, the physical flow model and computational formulation for the case are first examined and explained, then Comprehensive details of the computational calculations are examined for smooth pipe and non-interrupted grooved pipe. Moreover, the effect of axial groove at inner surface of tube is analyzed for the flow structure and thermal heat performance characteristics.

## PHYSICAL MODEL

Figure 1 demonstrates the grooved inner surface of the circular tube heat exchanger. The grooves arrangement and positions in the circular tube is specified in this figure. The geometrical structure specifications are employed in the tube, comprising 1920 mm tube-length, 11.08 mm tube-diameter, 2 mm tube-thickness, and  $1 \times 0.5$  mm groove-width and thickness along the axial direction. Temperature of inlet water is 313.15 K with a variation of Reynolds number between 1,500 and 23,000.

## COMPUTATIONAL SETUP

Complex flow features can be modeled using the Computational Fluid Dynamics, and the output can be displayed in a way that allows for comparison and visualization with actual flow data. In this work, ANSYS Fluent 2023R1 software is used to model the complex flow in a pipe with various geometrical configurations.

## Governing Equations

The mass, momentum and energy equation for incompressible, stead-state, Newtonian fluid are given below. Continuity equation:

$$\nabla \cdot \mathbf{V} = 0 \quad (1)$$

Where,  $\mathbf{V}$  is velocity vector and  $\nabla$  is the del operator in 3D special coordinate system.

Momentum Equation:

$$\rho(\nabla \cdot \mathbf{V})\mathbf{V} = -\nabla P + \mu \nabla^2 \mathbf{V} \quad (2)$$

Where,  $P$  is the pressure,  $\mu$  is Dynamic Viscosity and  $\rho$  is the density.

Energy Equation:

$$\rho C_p(\nabla \cdot \mathbf{V})T = \mu \Phi + K \nabla^2 T \quad (3)$$

Where,  $K$ ,  $C_p$ , and  $\Phi$  are the thermal conductivity, specific heat, and viscous dissipation function respectively.

## Description of Geometry

Figure 1 demonstrates both geometries for smooth and grooved tube. The top right image represents the smooth tube geometry for computational model. The geometry is a cylindrical shape structure with length of 1920 mm and width of 11.08 mm. The bottom left image represents grooved tube with the dimensions from Table 1.

**TABLE 1.** Dimensions for geometry.

Description	Dimension
Length	1920 mm
Width	11.08 mm
Groove-height	0.5 mm
Groove-width	1 mm

## Mesh Generation

Figure 2 describes the grid flow domains in physical space coordinates where the 3D coordinate tube system is implemented. In this current work, prism-shaped grids are successfully generated for smooth and axial groove geometries. It is essential to have more than adequate cell numbers to capture a good resolution; however, the requirement for memory increases. Careful verification of Grid independence is done in computer calculations for different grid numbers, such as 0.5 million, 1.5 million, 2.5 million, and 3.5 million cells, to ensure the validity and accuracy of the numerical results displayed in Table 2. The grid element system of 2.5 million is assessed and selected for examination in relation to this study in terms of accuracy and computational cost.

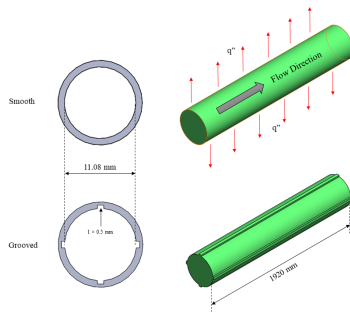


**FIGURE 1.** Smooth and groove tube configurations.

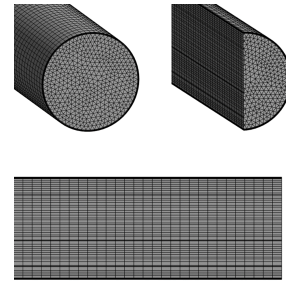


**FIGURE 2.** Mesh generation for flow domain in the pipe.

**TABLE 2.** Mesh independent study.

No. of elements	Heat Transfer Rate (W)	
	Present study	Exp. work
0.5 million	918.44	937
1.5 million	927.23	937
2.5 million	935.08	937
3.5 million	935.47	937

## Generating Mesh at Boundary Layer

To capture good resolution at the boundary layer, the mesh at the boundary should be more refined. A measure for boundary layer accuracy is called  $y^+$  study. For a good boundary layer resolution the value of  $y^+$  should be less than 2. The first cell height for each flow rate can be calculated using equation , with  $D = 11.08$  mm. The first layer thickness (in m) for case 1-4 was;  $2.05E-4$ ,  $4.10E-5$ ,  $2.34E-5$  and  $1.66E-5$ . The main tool used to refine the initial mesh was an inflation layer. The maximum element size was set to 0.5 mm to limit the size of the prism-shaped cells in the centre of the tube.

$$y_1 = D \times y^+ \sqrt{74Re}^{-\frac{13}{14}} \quad (4)$$

## Turbulence Modeling

The Reynolds number for the upper flow rate is highly turbulent and therefore a turbulence model is required to accurately represent the flow conditions. Accuracy at the wall boundary was considered highly important to capture convection between the tube wall and the fluid. The SST model was designed to provide more accurate predictions of flow separation close to the wall boundary. Hence, the SST model was selected for the simulations. To ensure convergence, a residual target of  $1 \times 10^{-6}$  was chosen for all equations in the heat transfer simulation, in addition, user points at the inlet and outlet monitored the temperatures.

The turbulence kinetic energy,  $k$ , and the specific dissipation rate,  $\omega$ , are obtained from the following transport equations:

$$\frac{\partial}{\partial t}(\rho k) + \frac{\partial}{\partial x_i}(\rho k u_i) = \frac{\partial}{\partial x_j} \left( \Gamma_k \frac{\partial k}{\partial x_j} \right) + G_k - Y_k + S_k + G_b \quad (5)$$

and,

$$\frac{\partial}{\partial t}(\rho \omega) + \frac{\partial}{\partial x_i}(\rho \omega u_i) = \frac{\partial}{\partial x_j} \left( \Gamma_\omega \frac{\partial \omega}{\partial x_j} \right) + G_\omega - Y_\omega + D_\omega + S_\omega + G_{\omega b} \quad (6)$$

In these equations,  $G_k$  represents the generation of turbulence kinetic energy due to mean velocity gradients.  $G_\omega$  represents the generation of  $\omega$ .  $\Gamma_k$  and  $\Gamma_\omega$  represent the effective diffusivity of  $k$  and  $\omega$ , respectively.  $Y_k$  and  $Y_\omega$  represent the dissipation of  $k$  and  $\omega$  due to turbulence.  $D_\omega$  represents the cross-diffusion term.  $S_k$  and  $S_\omega$  are user-defined source terms.  $G_b$  and  $G_\omega$  account for buoyancy terms.

The effective diffusivities for the SST  $k - \omega$  model are given by,

$$\Gamma_k = \mu + \frac{\mu_t}{\sigma_k} \quad (7)$$

$$\Gamma_\omega = \mu + \frac{\mu_t}{\sigma_\omega} \quad (8)$$

where,  $\sigma_k$  and  $\sigma_\omega$  are the turbulent Prandtl numbers for  $k$  and  $\omega$ , respectively. The turbulent viscosity,  $\mu_t$ , is computed by combining  $k$  and  $\omega$ , these equations are described in the Ansys Fluent Theory Guide [6].

## Boundary Conditions

The tube is 1.92 m in length with a 11.08 mm inner diameter. The fluid properties were based on Table 3 and the boundary conditions for were based on the following assumptions for simplification of the problem;

1. Inlet temperature of fluid is 313.15 K.
2. The inlet velocity profile is fully developed and corresponds to case 1 to 4 flow rates in Table 4.
3. The wall thermal condition is set to convective heat transfer with heat transfer coefficient is set to  $800 \text{ W/m}^2 \text{ K}$  and the bulk temperature of the fluid external to the tube is constant along the entire length at 293.15 K.

**TABLE 3.** Fluid properties.

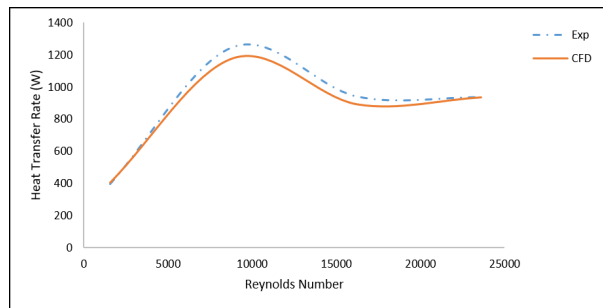
Property	Value	Unit
Density, $\rho$	992.32	$kg/m^3$
Specific Heat, $C_p$	4178	$J/kg \cdot K$
Thermal Conductivity, $k$	0.63	$W/m \cdot K$
Prandtl number, $Pr$	4.45	-
Dynamic Viscosity, $\mu$	6.71E-04	$N \cdot s/m^2$

**TABLE 4.** Flow rates.

Case No.	Flow Rate (l/min)	Reynolds Number
Case 1	0.56	1573
Case 2	3.15	8912
Case 3	5.74	16252
Case 4	8.33	23592

## VALIDATION OF COMPUTATIONAL RESULT

The current investigation follows a similar experimentation procedure described in Albanesi et al. [2]. This work carries out the crucial reliability validation of the conjugational calculations technique utilizing the CFD code. Therefore, for the smooth pipe, numerical technique validation is carried out by comparing the numerical data with the experimental one. The experimental results depended on the real performance of the heat exchanger tube. Detailed information concerning the pipe geometry configurations of a computational model for heat transfer rate for comparing data is represented in Figure 3. It is observed that there is good agreement between the numerical and experimental results. About 5% of the larger error variances are related to heat rate. Thus, by applying these numerical computations to model the fluid pattern and heat performance adequately in a circular tube with the interrupted groove, trustworthy computational results may be obtained based on this validation data.

**FIGURE 3.** Validation of a numerical model with available experimental data.

## RESULTS AND DISCUSSION

Figure 4 describes the velocity contours' variations for the smooth and grooved tube for different Reynolds Numbers. The significant flow change is continuous with the axial flow direction and occurs near to the axial groove. There are different mixing flow and counter-rotating flow vortices near the grooves. The flow behaves differently because more secondary flow is produced close to the groove channel, which displays streamlines in proximity groove channel wall. More pressure gradients in the flow direction are produced as a result of this change in inflow velocity. Therefore, when compared to a regular tube, all these modifications can enhance the heat performance in the grooved tube. These

results agreed with References [5].

Figure 5 represents the variations in temperature in both pipes (smooth and grooved). The figure illustrates that, using grooves can affect temperature distribution. These changes in temperature distribution lead to change in thermal boundary layers, leading to more improvement in overall thermal performance in the tube. These results agreed with References [13].

The influence of axial grooves on a pipe for thermal performance characteristics is obtained in terms of pressure drop and heat transfer rate for both smooth and grooved tubes with similar Re ranges. The differences in pressure drop against varying Re ranges for a smooth tube and grooved tube are shown in Figure 7. It is observed that the pressure drop within the tube increases with the increasing Reynolds number. Thus, the results showed that there are slight difference between the pressure drop in the smooth and the grooved tube, which means using groove has a very small effect on the pressure drop in the tube. The value of pressure drop for the grooved tube was higher than the smooth one, by about 0.168% - 1.68%.

Figure 6 illustrates the differences in heat transfer rate against varying Re ranges for a smooth tube and grooved tube. It is observed that the heat transfer rate within the tube increases with the increasing Reynolds number. Thus, the results showed that there are difference between the heat transfer rate in the smooth and the grooved tube, which means using groove has an positive effect on the heat transfer rate in the tube. The value of heat transfer rate for the grooved tube was higher than the smooth one, by about 2% - 10%. The overall thermal performance is increased with varying Reynolds number 1573, 8912, 16252, and 23592 is 12.91%, 6.78, 5.84%, and 7.32% respectively. It is evident from the results that highest overall performance occurs at low Reynolds number flows.

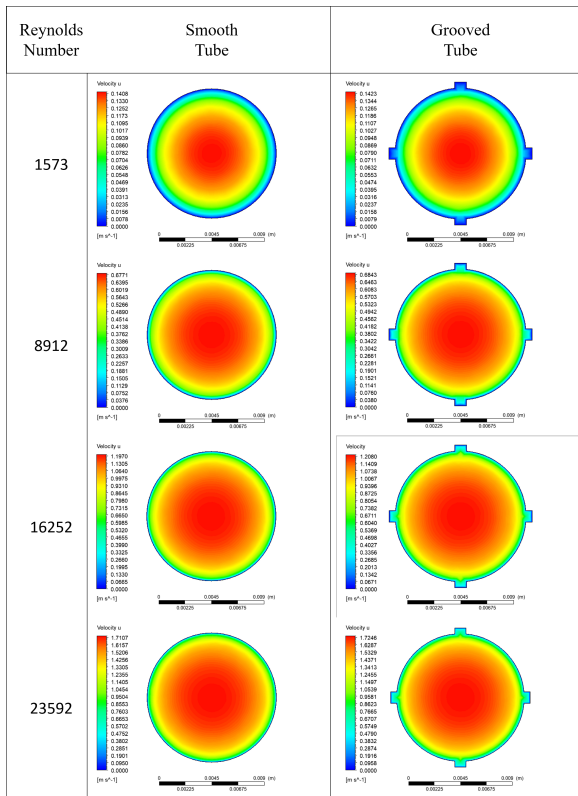


FIGURE 4. Velocity distributions.

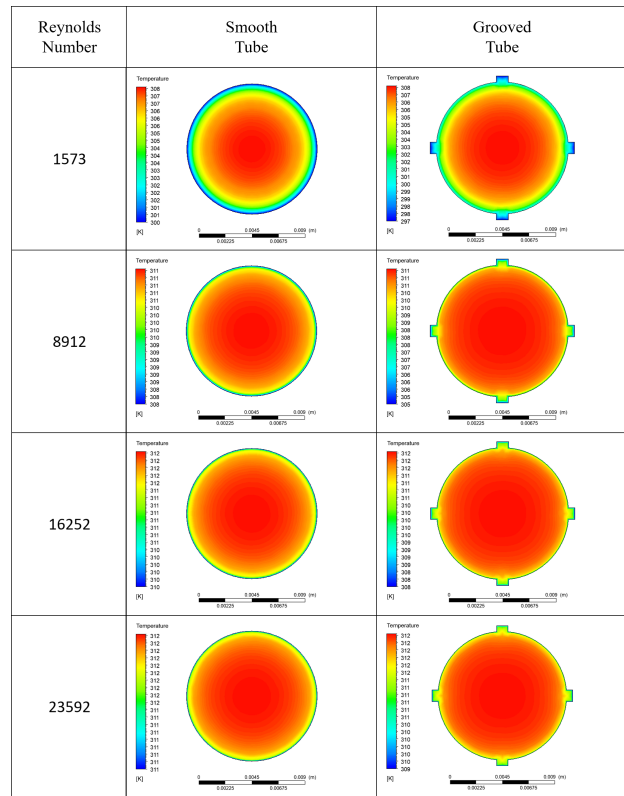


FIGURE 5. Temperature distribution.

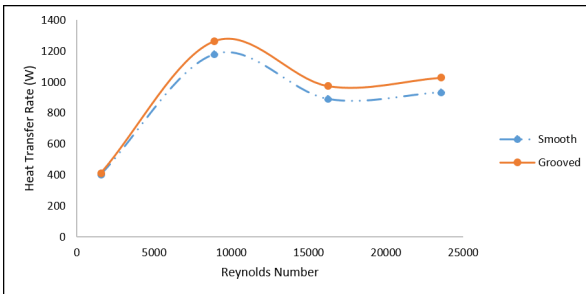


FIGURE 6. Comparison of heat transfer rate.

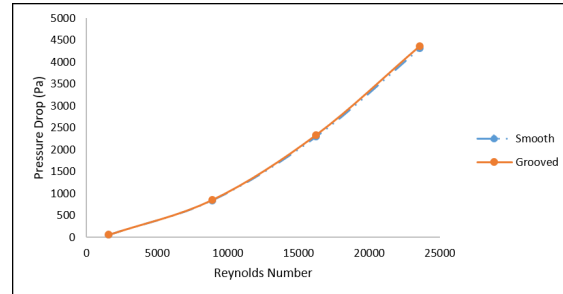


FIGURE 7. Comparison of pressure drop.

## CONCLUSION

In this investigation, characteristics of flow pattern and heat performance using a varying range of Reynolds number are analyzed numerically for smooth and grooved tube. This analysis is carried out to find the effect of overall heat transfer efficiency of the inner surface grooved tube. Based on this investigation the following conclusions can be drawn.

The numerical outcomes and experimental results are in good agreement. The higher error variance of the heat rate is about 5.59%.

The value of pressure drop for the grooved tube was higher than the smooth one for different Reynolds number, by about 0.168% - 1.68%.

The value of heat transfer rate for the grooved tube was higher than the smooth one for different Reynolds number, by about 2% - 10%.

The highest overall thermal efficiency increment is more than 12% for low Reynolds number at 1573.

## REFERENCES

1. S. M. Abolarin, M. Everts, and J. P. Meyer. Heat transfer and pressure drop characteristics of alternating clockwise and counter clockwise twisted tape inserts in the transitional flow regime. *International Journal of Heat Mass Transfer*, 133:203-217, 2019.
2. A. W. Albanesi, K. D. Daish, B. Dally, and R. C. Chin. Investigation of heat transfer enhancement in dimpled pipe flows. *In 21st Australasian Fluid Mechanics Conference Adelaide, Australia*, 2018.
3. Ahmed Ramadhan Al-Obaidi. Analysis of the flow field, thermal performance, and heat transfer augmentation in circular tube using different dimple geometrical configurations with internal twisted-tape insert. *Heat Transfer*, 49:4153-4172, 2020.
4. Ahmed Ramadhan Al-Obaidi and Jassim Alhamid. Numerical investigation of fluid flow, characteristics of thermal performance and enhancement of heat transfer of corrugated pipes with various configurations. *Journal of Physics: Conference Series*, 1733, 2021.
5. Ahmed Ramadhan Al-Obaidi, Jassim Alhamid, and Qasim Saleh. Analysis on flow structure and improvement of heat transfer in 3d circular tube with varying axial groove turbulator configurations. *Heat Transfer*, 50:1-16, 2021. <https://doi.org/10.1002/htj.22231>.
6. Inc. Ansys. *Ansys Fluent Theory Guide*. ANSYS, Inc., 2023.
7. P. Bharadwaj, A. D. Khondge, and A. W. Date. Heat transfer and pressure drop in a spirally grooved tube with twisted tape insert. *Int J Heat Mass Transfer*, 52:1938-1944, 2009.
8. K. Bilen, M. Cetin, H. Gul, and T. Balta. The investigation of groove geometry effect on heat transfer for internally grooved tubes. *Applied Therm Engineering*, 29:753-761, 2009.
9. S. Eiamsa-Ard, P. Nivesrangsan, S. Chokphoemphun, and P. Promvong. Influence of combined non-uniform wire coil and twisted tape inserts on thermal performance characteristics. *International Communications in Heat and Mass Transfer*, 37:850-856, 2010.
10. S. Eiamsa-Ard and P. Promvong. Numerical study on heat transfer of turbulent channel flow over periodic grooves. *International Communications in Heat and Mass Transfer*, 35:844-852, 2008.
11. M. Fiebig. Embedded vortices in internal flow: heat transfer and pressure loss enhancement. *International Journal of Heat Mass Transfer*, 16:376-388, 1995.
12. M. Mesgarpour, M. Bahiraei, S. Wongwises, A. Jodat, and O. Mahian. A cfd study of [c2mim][ch3so3]/al2o3 ionanofluid flow and heat transfer in grooved tubes. *Int J Thermophys*, 42:1-17, 2021.
13. Pongjet Promvong. Thermal enhancement in a round tube with snail entry and coiled-wire inserts. *International Communications in Heat and Mass Transfer*, 35:623-629, 2008.
14. F. Wu and W. Zhou. Numerical simulation and optimization of convective heat transfer and pressure drop in corrugated tubes. *Heat Transfer Research*, 43:527-544, 2012.